INSTITUTE OF PHYSICS PUBLISHING JOURNAL OF PHYSICS D: APPLIED PHYSICS

J. Phys. D: Appl. Phys. **39** (2006) 1594–1598 doi:10.1088/0022-3727/39/8/018

Multi-scale simulation of functionalization of rough polymer surfaces using atmospheric pressure plasmas

Ananth N Bhoj[1] **and Mark J Kushner**[2,3]

[1] Department of Chemical and Biomolecular Engineering, University of Illinois, Urbana, IL 61801, USA
[2] Department of Electrical and Computer Engineering, Iowa State University, Ames, IA 50011, USA

E-mail: bhoj@uiuc.edu and mjk@iastate.edu

Received 29 October 2005, in final form 10 February 2006
Published 30 March 2006
Online at stacks.iop.org/JPhysD/39/1594

Abstract
Atmospheric pressure discharges are routinely used to functionalize rough surfaces of commodity polymeric materials to enhance surface properties. High value polymeric materials, such as scaffolding for tissue engineering, must also have their surfaces treated to achieve similar functionality. The techniques used to achieve this functionality are typically costlier than the commodity processes used for bulk, web treatment of polymer sheets. The issue we are investigating is whether inexpensive, commodity plasma processes can be adapted to treat high value materials while considering the uniformity of processing on micro- and macro-scales. To address these issues a two-dimensional plasma hydrodynamics-surface kinetics model was developed and applied to the investigation of atmospheric pressure plasma functionalization of a polypropylene surface having microstructure using $He/O_2/H_2O$ mixtures. Non-uniformities in functionalization occur over both macroscopic and microscopic length scales and can be controlled by a judicious choice of O_2 fraction.

1. Introduction

Atmospheric pressure plasmas are routinely used to treat large areas of commodity polymer films (e.g. polypropylene(PP)) to improve surface properties such as adhesion and wettability [1] and to treat woven materials to improve water repellency [2]. Changes in surface properties occur by functionalizing a shallow surface layer (a few nanometres to 10 nm) by plasma generated species (radicals, ions and photons) thereby creating new functional groups on the surface but leaving the bulk polymer largely unaffected. Due to the commodity nature of these materials, the plasma processing must be inexpensive (a few cents m^{-2}). Typical plasma sources are atmospheric pressure coronae in a dielectric barrier configuration operating at a few kilohertz to tens of kilohertz having electrode separations of a few milimetres [3]. Polymer surfaces and textiles often have surface roughness that is characteristic of the material or results from the manufacturing process. The surface roughness can range from hundreds of nanometres to tens of μm [2, 3].

Biocompatible materials as used for implants [4], scaffolding for tissue engineering [5] and artificial skin [6] often have their surfaces treated to achieve similar functionality as commodity polymers to promote, for example, cell adhesion. These polymeric materials often have similar surface roughness to commodity polymers and woven materials. The techniques used to functionalize biocompatible materials are, however, typically more expensive than that for commodity materials.

The issue we wish to investigate is whether commodity plasma processes, such as functionalization by atmospheric pressure corona discharges, can be applied to the fabrication of high value biocompatible materials requiring high degrees of uniformity. In this regard, there are two spatial scales of interest. The first is macroscopic, a few tenths of a millimetre to a millimetre, defined by the extent or spacing

[3] Author to whom any correspondence should be addressed.

of the corona streamers. The second scale is on the order of the surface roughness, determined by the accessibility of plasma-generated species into the topography, or 'nooks and crannies', of the surface. Understanding the processes governing the uniformity of treatment on non-planar surfaces is therefore critical to adapting commodity techniques for high value materials. In this paper, we discuss results from a multi-scale, computational investigation of atmospheric pressure plasma treatment of polymer surfaces having microstructure. The investigation was conducted with a two-dimensional (2d) plasma hydrodynamics model [7], which was integrated with a surface kinetics model. The surface functionalization of PP in oxygen containing plasmas was studied. We found that non-uniformities in functionalization occur over both macroscopic and microscopic length scales. These non-uniformities can be controlled by a judicious choice of the O_2 fraction which also enables control of the surface coverage of different functional groups.

2. Reaction mechanism and model parameters

The model used in this investigation is a 2d hydrodynamics simulation [7] that solves the Poisson equation for electric potential simultaneously with the multi-fluid charged and neutral species conservation equations on an unstructured mesh. Updates of the charge particle densities are followed by an update of the electron temperature and neutral densities in a time-splicing manner. Gain and loss terms due to electron impact ionization and excitation, heavy particle reactions, photoionization, secondary emission and surface reactions are included. The surface kinetics model implements a surface site balance model at every point along the plasma-surface boundary.

The treatment of PP with microstructure was investigated in $He/O_2/H_2O$ corona discharges using the surface reaction mechanism developed for PP treatment in humid air [8]. The species considered in the gas phase mechanism include He, $He(^2S)$, He^+, O_2, $O_2(v)$, $O_2(a\,^1\Delta)$, $O_2(b\,^1\Sigma)$, O_2^+, O_2^-, O, $O(^1D)$, $O(^1S)$, O^+, O^-, O_3, O_3^-, H_2O, H_2O^+, H and OH. During the short (<5 ns) discharge pulse, electron impact excitation, ionization and dissociation dominate radical formation. In the interpulse periods (IP), the balance of reactive fluxes to the surfaces is dominated by three-body processes. The species that are largely responsible for surface functionalization include H, OH, O, O_2 and O_3, which are also created in humid air corona discharges [8].

Functionalization of the PP surface consists of adding O species to the surface to increase its surface energy and hence its wettability. The initiating step is the abstraction of H from the PP surface by O and OH radicals, creating surface alkyl radical sites (R–•, where R is the PP backbone). These sites further react with O and O_3 forming alkoxy radicals (R–O•). Alkyl radicals also react with OH radicals via a slower pathway to form alcohol groups (R–OH). Alkoxy radicals react at a slower rate with molecular O_2 to form peroxy radicals (R–O–O•) and at a faster rate by abstracting H from surrounding sites to form alcohol functional groups. The competing β-elimination type reaction of alkoxy radicals creates carbonyl groups (R=O), which further oxidize to form carboxylic acid groups (R=O(OH)). This scission pathway ultimately oxidizes the terminal carbon centres on the polymer backbone to create CO_2, which is a by-product of surface treatment.

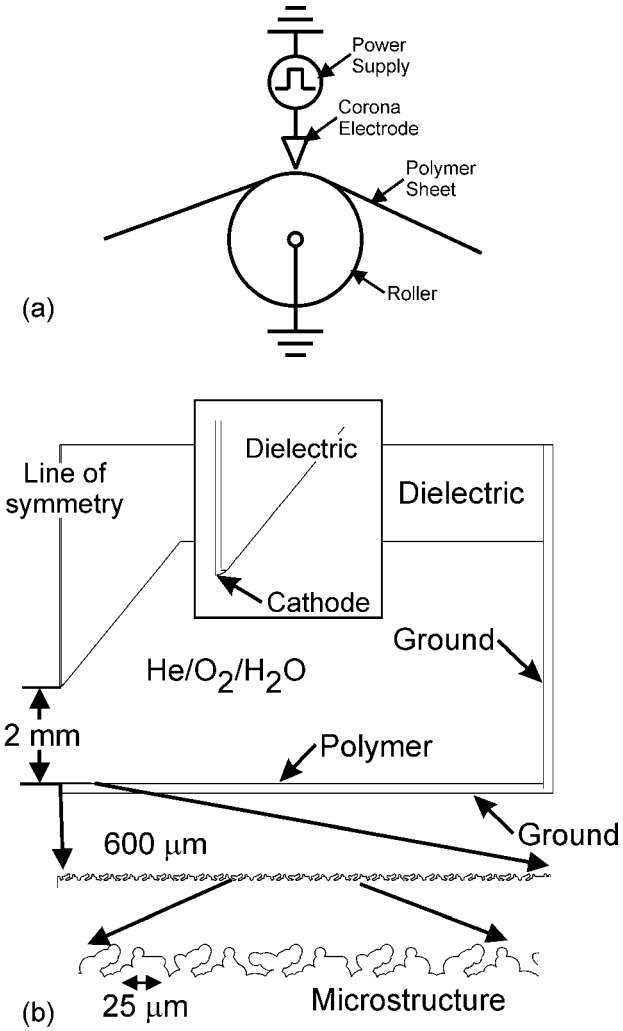

Figure 1. Schematic of the corona dielectric barrier discharge. (*a*) Web treatment of polymer sheets treated in a continuous manner by a powered corona source. (*b*) The linear corona cathode tip, shown in the inset, is 2 mm from the PP surface. Microstructure on the surface has features the sizes of a few microns.

The plasma source is a linear corona as used in web treatment of polymer sheets and is schematically shown in figure 1(*a*). Polymer sheets are fed at speeds of many metres per second over a grounded roller or drum. A linear corona discharge, pulsed at many to tens of kilohertz, has a gap of a few millimetres between the electrode and surface of the polymer. An enlargement of the electrode and near electrode structures is shown in figure 1(*b*). The upper wedge-shaped dielectric structure, symmetric across the centerline, has an embedded powered electrode exposed to the gas at the tip 2 mm above the PP surface. The PP surface is on the lower flat grounded electrode creating a dielectric barrier discharge configuration. Roughness on the polymer surface is resolved with strand-like features having many micron length scales. The unstructured numerical mesh simultaneously resolves both the reactor and microstructure length scales, a dynamic range of approximately 1000. There were

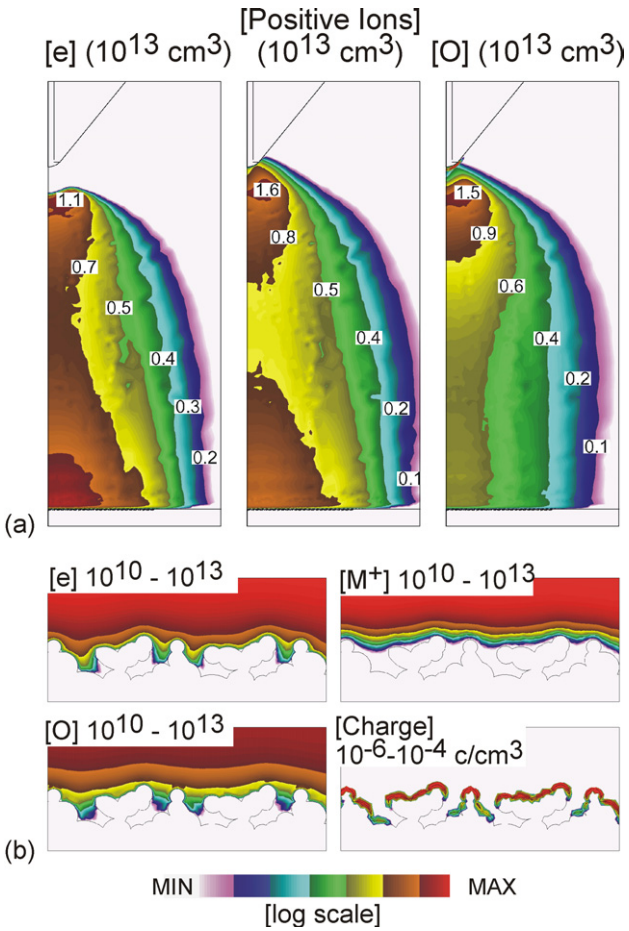

Figure 2. Plasma and surface properties after the avalanche closes the gap for $He/O_2/H_2O = 98/1/1$. The densities of [e], O atoms and positive ions are shown in the (*a*) bulk plasma and (*b*) near the surface (including surface charge). Charged species penetrate to a limited extent into surface features.

21 296 computational nodes in the mesh, including 9643 in the plasma.

3. Surface functionalization of polypropylene

The discharge is operated at a repetition frequency of 10 kHz by biasing the powered electrode with −5 kV, 10 ns pulses. Plasma dynamics, plasma chemistry, neutral gas phase chemistry and surface kinetics are fully resolved during the powered pulses. During the IP, only the neutral gas phase chemistry and surface kinetics are followed. Typical conditions in the bulk plasma and near the surface at the end of the discharge pulse 3.5 ns after initiation in an atmospheric pressure mixture of $He/O_2/H_2O = 98/1/1$ are shown in figure 2. The avalanche, terminated by charging of the PP dielectric, produces electron densities and ion densities of 10^{13} cm^{-3}, and densities of O atoms of 10^{13} cm^{-3}. As the avalanche approaches the surface, electrons penetrate inside surface features to a limited extent but withdraw due to surface charging. Surface features having large view angles to the plasma rapidly acquire a large negative charge, thereby preventing further penetration into the surface structure. Positive ions have similarly limited penetration due to the local ambipolar forces which constrain their transport. Neutral radicals such as O penetrate deeper inside the surface features by diffusion.

Surface treatment results from reactions with radicals such as O and O_3 during the IP for accumulated periods of tens to hundreds of milliseconds following tens to hundreds of discharge pulses. In the results discussed here, the densities of surface functional groups reached a steady state over few hundreds of milliseconds. The extent of functionalization was investigated as a function of O_2 fraction, $f(O_2)$, which in large part determines the ratio of the flux of O and O_3 to the surface. O atoms are efficient at initiating surface reactions by H abstraction. O_3 initiates the rapid pathway leading to the conversion of surface radicals to alcohol functional groups. The dependence of O fluxes to the surface is shown in figure 3(*a*) as a function of $f(O_2)$. At the end of the discharge pulse (start of the IP period), the O atom flux monotonically increases with $f(O_2)$ due to there being more electron impact dissociation of O_2. As $f(O_2)$ increases, however, the rate of conversion of O to O_3 also increases. As a result, there is little O atom flux to the surface at the end of the IP period with large $f(O_2)$. The O atoms have largely been converted to O_3.

Fluxes of O radicals and O_3 along the surface averaged over an IP period for $f(O_2)$ of 10% and 75% are shown in figures 3(*b*) and (*c*). There is a large-scale and a small-scale structure. The large-scale structure results from the spatial distribution of radicals incident onto the surface and the rate of conversion of O to O_3. At high $f(O_2)$, O atoms are more rapidly converted to O_3 and so the transport of O atoms is reaction limited. The flux of O is larger near the axis where the O atom production by electron impact is largest. At low $f(O_2)$, both the production of O atoms and the rate of conversion to O_3 are lower but the O atoms are more mobile, thereby producing more uniform fluxes on a macro-scale. The small-scale structure results from the ability of O, OH and O_3 to penetrate into the microstructure of the film. On a micro-scale, there is a ±30–40% variation in the fluxes to the surface. Protruding tips with larger view angles to the plasma receive larger fluxes of O and O_3 than the recesses of the surface structure.

Alcohol function groups, (R–OH), are formed under humid conditions where there is a reasonable flux of O atoms and a significant flux of OH radicals. The reaction sequence begins with abstraction of H from R–H by O or OH to form alkyls, R–•. In the absence of large O atom fluxes, the alkyl sites are passivated by O_2 to form peroxy sites, R–O–O•, which react with OH to yield R–OH on longer timescales. With moderate O-atom or O_3 fluxes, alkyl sites are passivated to form alkoxy sites, R–O•, which in turn abstracts H atoms from surrounding sites to form R–OH sites. With abundant formation of R–O•, the formation of R–OH by this surface–surface process is very rapid on timescales of tens of milliseconds. A secondary H abstraction reaction of R–OH by O atoms reforms alkoxy sites. One should therefore expect large alcohol functionalization for conditions that provide moderate fluxes of O and OH and low O_2 fluxes.

The surface coverages of alcohol [s(R–OH)], peroxy [s(R–O–O•)] and alkoxy [s(R–O•)] functional groups for different $f(O_2)$ after a treatment time of 1 s are shown in figure 4(*a*).

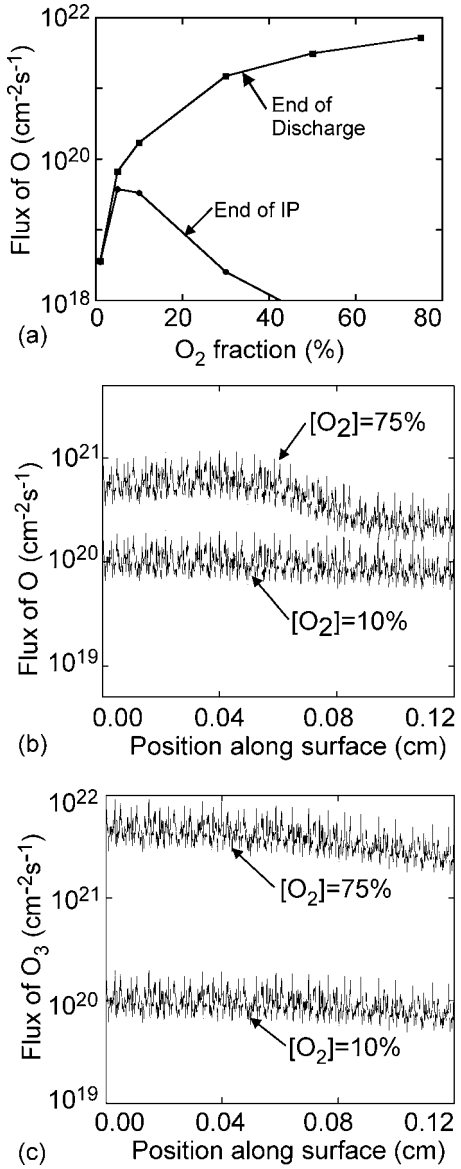

Figure 3. Fluxes of O and O_3 to the surface. (*a*) O-atom fluxes at the end of the discharge pulse (start of IP) and at the end of the IP at a position 0.05 cm along the surface from the axis. (*b*) O-atom fluxes along the surface averaged over an IP for $f(O_2)$ of 10% and 75%. (*c*) O_3 fluxes along the surface averaged over an IP for $f(O_2)$ fractions of 10% and 75%.

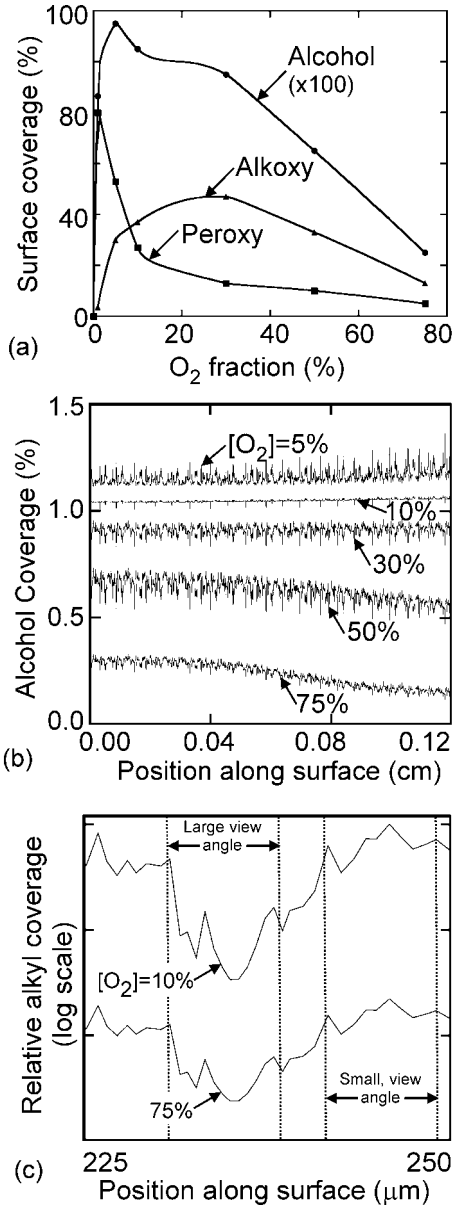

Figure 4. Surface functionalization for different $f(O_2)$. (*a*) Average surface coverage of alkoxy, peroxy and alcohol functional groups after 1 s treatment. (*b*) Coverage of alcohol groups with position along surface after 1 s treatment. (*c*) Surface coverage of alkyl radicals after 0.05 s treatment for $f(O_2)$ 10% and 75%.

Due to the large fluxes of O_2 at any finite $f(O_2)$, s(R–O–O•) will exceed s(R–OH). The ratio between s(R–O–O•) and s(R–OH) can, however, be controlled by $f(O_2)$. At low $f(O_2)$, alkyl sites are passivated into predominantly peroxy rather than alkoxy, R–O•, groups due to there being low fluxes of O_3 which would otherwise form alkoxy sites. As $f(O_2)$ decreases, more discharge energy is expended in the dissociation of H_2O rather than O_2, thereby increasing OH fluxes. The larger rate of H abstraction by OH followed by passivation by O_2 results in s(R–O–O•) being maximum at approximately $f(O_2) = 0.01$. Also, as $f(O_2)$ decreases, which increases the fluxes of OH, s(R–OH) increases reaching a maximum at $f(O_2) = 0.05$. s(R–OH) decreases at lower values of $f(O_2)$ primarily because the formation of alkoxy sites decreases due to the lower fluxes of O_3. This reduces R–OH formation through the surface–surface reaction of R–O• abstracting H from an adjacent surface site.

As $f(O_2)$ increases beyond 5–10%, the fluxes of O and OH decrease while the flux of O_3 increases. The rate of formation of R–O–O• is lower, being replaced by formation of R–O• due to the larger flux of O_3. Higher O_3 fluxes convert available alkyl sites into alkoxy groups which predominate over peroxy groups. In spite of the larger s(R–O•), the availability of alkyl sites is rate limiting and so the formation of s(R–OH) by OH passivation decreases. As $f(O_2)$ increases beyond 30%, the creation of alkyl sites is the rate limiting step and s(R–O•) decreases.

s(R–OH) as a function of position for different $f(O_2)$ after a treatment time of 1 s are shown in figure 4(*b*). The

macro-scale variations in s(R–OH) at large f(O_2) are due to spatial gradients in radical fluxes, predominantly O, that make alkyl sites the precursor to R–OH. Micro-scale variations in s(R–OH) are most significant at very low and higher f(O_2). The uniformity of coverage is best at f(O_2) of 10%. This variation is ultimately tied to the disposition of alkyl sites. At very low f(O_2), alkyl sites are saturated into peroxy groups that contribute to alcohol formation and increase micro-scale non-uniformities. At higher f(O_2) higher O_3 fluxes rapidly convert alkyl to alkoxy sites, thereby eliminating the R–OH precursor. The transport of O_3 is therefore important to the uniformity of functional groups on a micro-scale. For example, alkyl coverage along the surface after 0.05 s of treatment is shown in figure 4(*c*). The locations that have smaller alkyl coverage are at the tips of the surface structure. These are sites that have larger view angles and receive larger fluxes of O_3 which passivates alkyl sites.

4. Concluding remarks

In conclusion, the functionalization of PP surfaces having microstructure by atmospheric corona discharges sustained in He/O_2/H_2O mixtures was investigated using a 2d multi-scale model. Non-uniformity in functionalization on macro- and micro-scales is attributed to temporal and spatial variations in reactive fluxes, their ability to penetrate into the microstructure and the disposition of surface radical sites. In low f(O_2) mixtures, secondary reactions of peroxy groups with OH radicals increase micro-scale non-uniformities. With intermediate f(O_2) mixtures, about 10%, the flux of O atoms is more uniform and the formation of O_3 is low. As a result functionalization is more uniform on both macro- and micro-scales. With higher f(O_2), transport limitations for O atoms and the formation of reactive O_3 results in larger variations in functionalization between surface sites that have large and small view angles to the plasma.

Acknowledgments

This work was supported by the National Science Foundation (CTS-0520368) and 3M Inc. The authors thank Dr Mark Strobel for his advice during this research.

References

[1] Chan C-M 1994 *Polymer Surface Modification and Characterization* (New York: Hanser/Gardner)
[2] Borcia G, Andersonrown C A and Brown N M D 2003 *Plasma Sources Sci. Technol.* **12** 335
[3] Strobelrown J M, Strobel M, Lyons C S, Dunatov C and Perron S J 1991 *J. Adhes. Sci. Technol.* **5** 119
[4] Chim H, Ong J L, Schantz J-T, Hutmacher D W and Agrawal C M 2003 *J. Biomed. Mater. Res.* **65A** 327
[5] Nitschke M, Schmack G, Janke A, Simon F, Pleul D and Werner C 2002 *J. Biomed. Mater. Res.* **59** 632
[6] Beumer G J, van Blitterswijk C A and Ponec M 1994 *J. Mater Sci: Mater. Med.* **5** 1
[7] Bhoj A N and Kushner M J 2004 *J. Phys. D: Appl. Phys.* **37** 2510
[8] Dorai R and Kushner M J 2003 *J Phys. D: Appl. Phys.* **36** 666